Available online at www.sciencedirect.com
ScienceDirect
Journal of Power Sources 168 (2007) 307–322
JOURNAL OF POWER SOURCES
www.elsevier.com/locate/jpowsour

The anode efficiency in methanol direct fuel cells—A chronoamperometric approach

M. Ohanian [a], C.F. Zinola [b,*]

[a] *Chemical Engineering Institute, School of Engineering J. Herrera y Reissig 565, Universidad de la República, Montevideo, CP 11300, Uruguay*
[b] *Fundamental Electrochemistry Laboratory, School of Sciences, Iguá 4225, Universidad de la República, Montevideo, CP 11400, Uruguay*

Received 29 December 2006; received in revised form 27 February 2007; accepted 28 February 2007
Available online 7 March 2007

Abstract

The methanol oxidation reaction has been studied on polycrystalline platinum surfaces, cathodically treated platinum and platinum surfaces modified by a second (or a third) metal deposited spontaneously in 0.50 M methanol + 0.5 M sulphuric acid using chronoamperometry. The electrochemical behaviour of methanol on the three types of electrodes shows that the initial oxidation rate is higher on the cathodically treated electrodes, whereas it depends on the nature of the second spontaneously deposited metal; silver shows inhibition and ruthenium and osmium exhibit a catalytic behaviour for the same 20% amount of surface metal ad-atoms.

Analysis of the methanol chronoamperometric data show that the steady-state current, recorded after 3000 s, is larger for the cathodic treated surfaces than for bare platinum. Moreover, the initial slope of the current versus time plot is positive for both surfaces, that is, the competition between carbon monoxide formation and methanol first oxidation occurs. On the other hand, methanol oxidation on platinum modified by spontaneously deposited metals always exhibits negative signs in the initial current versus time slopes, independent of the nature of the metal ad-atom.

A theoretical analysis of the kinetic laws for methanol electrocatalytic oxidation is presented. The fitting of the chronoamperometric data with the mathematical model, allows the discussion of methanol decomposition, carbon monoxide oxidation and direct methanol oxidation on the different surfaces. The time dependent expression of the surface coverage by methanol adsorbates is also derived and the characteristic values of the reaction are calculated for the different platinum electrodes. The potential dependences of parameters directly related to the electrochemical rate constants of the each step were also evaluated.

Keywords: Methanol; Fuel cells; Chronoamperometry; Theoretical models; Anodes

1. Introduction

Global warming due to greenhouse gases has been a worldwide problem since the late seventies. In order to decrease pollutant levels, advances in electric vehicles that produce negligible amounts of harmful emissions and show efficiency improvements are essential. Fuel cells are promising power generation systems of high efficiency since they are able to convert the free energy change of a chemical reaction directly into electrical energy. Although an attractive strategy, it is obvious that improving the efficiency of current systems alone will not be sufficient to meet the Kyoto targets [1]. In the case of low temperature fuel cells the selected fuel is hydrogen. However, the ability of hydrogen to compete economically as a transportation fuel rests primarily on reduction of the fuel-cycle cost and storage methods [2].

One of the most popular liquid fuels is methanol, and there is great interest in its direct oxidation without a previous reforming step in the so-called direct methanol fuel cell (DMFC). One of the obstacles to overcome in making a DMFC practical is the lack of efficient poison-tolerant anode catalysts [3]. In the oxidation of methanol on platinum, surface carbon monoxide is formed as a stable product, which blocks catalytic sites and inhibits further methanol oxidation. Therefore, a good anode catalyst for DMFC must transform the poisonous carbon monoxide into free carbon dioxide using oxygen atoms available in the interfacial water or in the water decomposition products such as adsorbed hydroxyl species. This leads to the release of surface sites for

* Corresponding author. Tel.: +59 82 525 07 49; fax: +59 82 525 07 49.
E-mail address: fzinola@fcien.edu.uy (C.F. Zinola).

0378-7753/$ – see front matter © 2007 Elsevier B.V. All rights reserved.
doi:10.1016/j.jpowsour.2007.02.072

a catalytic methanol oxidation. In this sense, platinum surfaces have been modified either with highly reductive potential programs or with the deposition of ad-metals to change the carbon monoxide surface binding properties and lessen the effect of the carbon monoxide poisoning [4].

Although the decomposition and oxidation reactions of methanol on platinum have been studied extensively in the past, the exact mechanism that explains the observed experimental facts still remains unclear. It has been studied by Bagotzki and Vassiliev [5] on polycrystalline (pc) platinum at different electrode potentials, pH and bulk concentrations. They found that the decrease in the chronoamperometric transients were due to the increase in the surface coverage by adsorbed methanol. They also analysed the kinetic currents at different degrees of coverage by hydroxyl and carbonaceous species, making visible the surface recombination between the two adsorbates as rate-limiting step for potentials below 0.70 V versus RHE. Steady-state Tafel lines for methanol oxidation were used to analyse the change in the slopes considering different values of surface coverages by methanol. A similar analysis was performed by Indara et al. [6] for both methanol and hydroxyl adsorbates.

Technological studies of methanol oxidation at different anodes in a DMFC shows that an increase in platinum loading to 5–10 mg cm^{-2} is required to obtain the desired output current and potential in comparison with the 0.2–0.5 mg cm^{-2} on supported carbon catalysts [7]. The co-deposition of two or more active metals in a new binary alloy catalyst lowers metal loadings and then, the cost of the catalysts. According to previous papers [8–11] it seems that the most convenient electrocatalyst is the platinum/ruthenium alloy that can be prepared according to different methodologies; painting, spraying or ink printing, emulsions, electrodeposition, etc., over a carbon support [12,13]. Stab and Urban [14] have patented an archive covering noble metal and binary alloy deposition methods using sixteen metallic salts as anodes for a DMFC. It has been proposed that potential programs of different wave signals are the most adequate to obtain selected morphologies with frequencies down to 100 kHz. One simple method that does not require any sophisticated equipment is the spontaneous deposition previously studied by us [15] and it is the one used in this paper.

Considering the case of methanol oxidation mechanism on bimetallic surfaces, the “bifunctional mechanism” and the “ligand effect theory” can explain the results. However, it has been demonstrated that the first mechanism contributes more than two-thirds of the overall effects found for methanol oxidation on platinum/ruthenium. Using the Polanyi relationship, it was possible to calculate that the process only changes in 40 mV due to the ligand effect of the ca. 200 mV shift in the onset oxidation potential towards the negative direction [6]. Gasteiger et al. [7] used different proportions of bulk platinum/ruthenium alloys in acid solutions to approach the chronoamperometric transients at low methanol concentrations. Other authors [12] use chronoamperometric plots for only qualitative purposes between the catalytic activity of bare platinum, platinum/ruthenium and platinum/tin. Herrero et al. [13] use the current at zero time as criteria in chronoamperometry to further obtain Tafel lines on Pt(1 1 1), Pt(1 1 0) and Pt(1 0 0) in sulphuric, perchloric and phosphoric media. They also analysed in UHV conditions with radiotracer methods the mechanism of methanol oxidation electrocatalysis with a kinetic law to model the chronoamperometric curves. The total current was considered as the addition of the double layer current contribution, continuous methanol oxidation component and seudocapacitive methanol adsorption current [12,13]. They solve the equations for different reaction orders for surface methanol species from one to four, founding the best fitting for the second order.

On the other hand, a reaction mechanism has been proposed taking a single carbonaceous adsorbed species with further reactions including various types of hydroxyl adsorbates [16]. They assume that hydroxylates are fast and reversibly produced and then, their surface coverage can be almost constant at any reaction operation time. They fit their experimental curves with a proposed model finding good correlation. Ishikawa et al. [17] developed a theoretical study for methanol electrooxidation mechanism using the adsorption energy of the intermediate adsorbates by the bond energy of the metal atoms. They found that the first methanol dehydrogenation is favourable, but not the presence of water-discharged products, which are determining in the oxidative desorption of carbon monoxide. They also found that the presence of adsorbed water on ruthenium atoms is more favourable than on platinum atoms.

Based on the reaction scheme for methanol oxidation, it is clear that the ratio and distribution of platinum and ruthenium catalyst sites influences the methanol oxidation kinetics [18,19]. In spite of being the optimal surface distribution of both metals 50:50 (as predicted by the Langmuir–Hinshelwood mechanism) it has been shown that catalysts consisting of homogenously distributed surface sites of 70–30 atomic percent (at.%) platinum to ruthenium ratio display the best activity for methanol oxidation reaction [20].

The nature of the chemical state of the ruthenium ad-metal component has also been suggested to influence the methanol oxidation kinetics [21]; however, there is disagreement regarding the most active form of ruthenium. It has been reported to be significantly poorer (ca. 250 times lower) for methanol oxidation when catalysts consisted of mixtures of platinum and ruthenium-oxides [22]. Based on these results, it was recommended that platinum/ruthenium alloys should not be used for direct methanol fuel cells [23]. In subsequent studies [24,25], it was suggested that ruthenium in its metallic state is most active for methanol oxidation. They based their conclusions mainly on adsorbed carbon monoxide to carbon dioxide oxidation studies for hydrogen-reduced catalysts. XPS was used to obtain the chemical state of ruthenium immediately before and after methanol oxidation [25]. It was shown that ruthenium-oxides are partially reduced to metallic ruthenium in the electrochemical environment [26] during the course of the reaction.

However, it is important to notice that some earlier results on well-characterized platinum electrodes suggest that, under certain conditions, carbon dioxide production from methanol electrooxidation can occur by a non-carbon monoxide pathway i.e. the parallel pathway [27]. In a potentiostatic methanol oxidation it was also observed carbon dioxide production on

both Pt(1 0 0) and Pt(1 1 1) at potentials where adsorbed carbon monoxide is surface stable [28,29]. Direct evidence for carbon dioxide production at low potentials comes from *in situ* IR spectroscopy measurements on both Pt(1 1 1) and Pt(1 0 0) electrodes [30]. The inferences from these studies were confined to potentials where adsorbed carbon monoxide did not oxidize to carbon dioxide. On the other hand, chronoamperometric measurements on Pt(1 1 1) at 0.6 V versus RHE extended these results and showed that the parallel path was active even when adsorbed carbon monoxide oxidizes to carbon dioxide [31]. The parallel path accounted for more than 75% of the total carbon dioxide produced under steady state conditions [31]. In reality, methanol electrooxidation consists of several elementary reactions each of which may not only occur at different rates under unsteady state conditions, but also respond differently to residue accumulation. A model that successfully accounts for these transient effects must include further details of the surface reactions and not precisely using the parallel mechanism premise.

In this paper, we develop a series kinetic model for methanol electrooxidation based on our current understanding. A theoretical analysis based on the electrocatalytic kinetic law for methanol oxidation is presented. The fitting of the chronoamperometric data is compared with the mathematical model and methanol decomposition and carbon monoxide oxidation are discussed on the basis of experimental and theoretical results. We analysed the model predictions with chronoamperometric data for acidic methanol oxidation on bare and cathodically treated platinum and on platinum modified by ruthenium, osmium and silver.

2. Experimental

Electrochemical experiments were performed at 20 °C in a micro flux three-electrode cell using different pc platinum wires (0.5 mm diameter, 99.999% purity from Goodfellow Co.) as working electrodes. The electrochemical set-up was completed using a large-area-platinum counter electrode and a reversible hydrogen reference electrode (RHE). The 0.5 M sulphuric acid supporting electrolyte was prepared from J.T. Baker reagent with MilliQ*-Millipore treated water (18.2 MΩ cm of resistivity). All potentials in the text are referred to the RHE scale.

Smooth platinum working electrodes were immersed first in hot concentrated sulphuric acid:nitric acid solution for half an hour, then repeatedly rinsed in Milli-Q* water and finally placed in the supporting electrolyte. Chemically cleaned platinum electrodes were electrochemical activated firstly by a 20 min potential holding at 2.0 V in 0.5 M sulphuric acid solution, secondly and after the solution was replaced by fresh supporting electrolyte, repetitive 2.5 V s^{-1} scans were run for 20 min and finally stabilized electrode by 15 min of potential cycling at 0.10 V s^{-1} between 0.035 and 1.50 V. The real surface area of working electrodes was ca. 0.30 cm^2, which were calculated from the hydrogen ad-atom voltammetric integration after double layer correction.

The 0.5 mM ruthenium-containing solution was prepared from $RuCl_3 \cdot 3H_2O$ (Aldrich–Sigma), the 0.5 mM osmium-containing solution from $OsCl_3 \cdot xH_2O$ (Aldrich–Sigma) and the 0.1 mM silver-containing solution from silver sulphate (Merck) all in 0.2 M sulphuric acid solutions. They were used as a source of ruthenium, osmium and silver aqua-complex, prepared without local large salt concentrations to avoid precipitations and polymerisation. For spontaneous deposition, the immersion time (considered as the time in contact with the metal-containing solution) for ruthenium was 120 s and for osmium and silver was 60 s under a nitrogen atmosphere. The calculation of the degree of surface coverage (θ_{Me}) by the foreign metal on pc platinum reaches 0.20–0.25 ML and was conducted by the integration of the voltammetric profile of the interface in the hydrogen adsorption region after double layer correction according to Eq. (1).

$$\theta_{Me} = \frac{Q_H^o - Q_H}{Q_H^o} \quad (1)$$

Q_H^o and Q_H being the hydrogen ad-atom charge density before and after metal deposition, respectively.Sometimes a solution composed by 0.5 mM ruthenium-cation + 0.5 mM osmium-cation in 0.2 M sulphuric acid was used to prepare the ternary platinum/ruthenium/osmium surfaces. The immersion time (t_{dep}) was 60 s. The stabilization of the spontaneous deposition on platinum was performed, after washing the electrode with supporting electrolyte, by not more than six potential cycles in the hydrogen ad-atom region at 0.10 V s^{-1} until repetitive scans can be obtained.

The cathodically treated platinum working electrodes were prepared by applying a potentiostatic signal (PS) in 0.5 M sulphuric acid. Platinum was subjected to this PS at a preset potential, E, of −1.0 V during 5 min under a continuous bubbling of the solution. The excess of molecular hydrogen at the electrode was removed by 15 min at 0.05 V under vigorous nitrogen bubbling. In all cases the repetitive voltammetric response of the resulting surface was run from 0 to 1.55 V at 0.10 V s^{-1} immediately afterwards to check the surface area of the working electrode.

The 0.5 M methanol + 0.5 M sulphuric acid working electrolyte was prepared from pure methanol (Merck reagent) with MilliQ*-Millipore water. Methanol solution oxidation was studied by chronoamperometric plots during 3000 s in the working electrolyte with a sample frequency of 2 Hz, at different selected potentials on each platinum surface.

3. Results

3.1. Platinum modified surfaces by cathodic treatments: methanol bulk oxidation

We prepared a freshly reduced platinum active surface by cathodic polarisation. Burke and Hurley [32] discussed the effect of platinum activation by thermal pre-treatment. He pointed out that, three active states of platinum are involved, which explained the three anodic peaks in the first positive anodic sweep in acid solution (0.75, 0.45 and 0.25 V).

Fig. 1 shows the current versus potential response of a cathodically treated surface with PS of different E from −1.5 to 0 V. The voltammetric response shows the following unusual

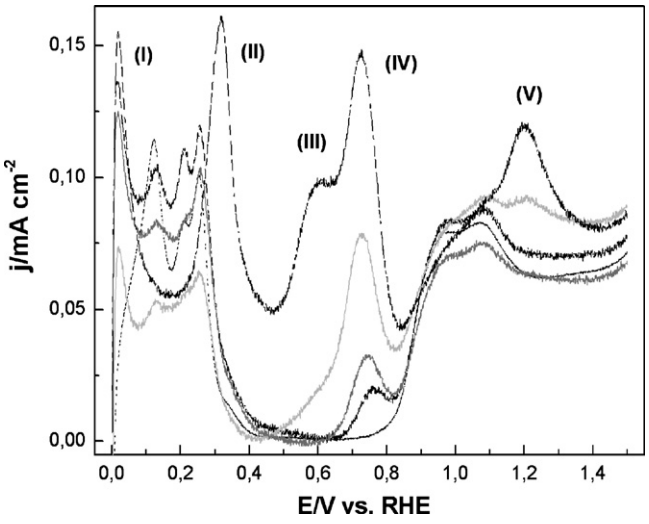

Fig. 1. Cyclic voltammetric profile of pc platinum (dotted line) run between 0.05 and 1.55 V at 0.10 V s^{-1} in oxygen free 0.5 M sulphuric acid solution at room temperature. The CT procedure is applied to the platinum electrode as explained in the text; $E = 0$ V (continuous line), $E = -0.5$ V (dark grey line), $E = -1.0$ V (light grey line), $E = -1.5$ V (dashed line).

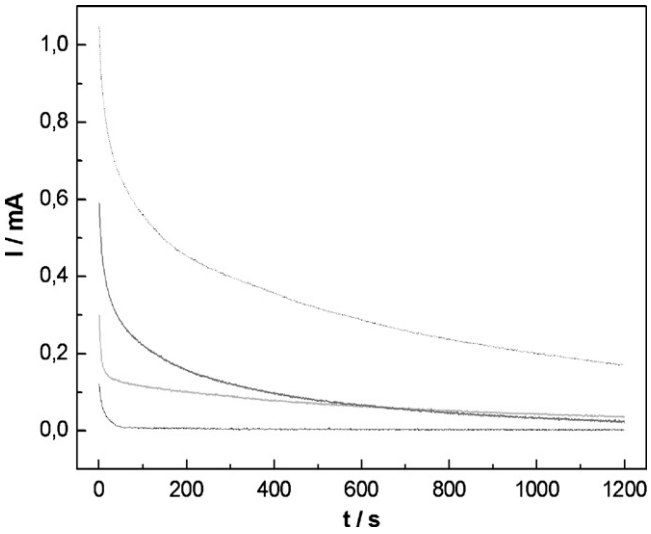

Fig. 2. Chronoamperometric plots for methanol oxidation on bare platinum recorded at different electrode potentials in oxygen free 0.50 M methanol + 0.5 M sulphuric acid; 0.40 V (continuous line), 0.65 V (light grey line), 0.70 V (grey line), 0.775 V (dotted line).

features in the positive going potential sweep; a total depletion of the hydrogen ad-atom region and three anodic signals assigned to hydrogen and hydroxyl subsurface oxidation formed on more labile platinum active sites of lower coordination indices (located at ca. 0.3, 0.6, and 0.75 V) [33]. Moreover, at 1.2 V another anodic peak is observed associated with an oxygen-containing species of a less labile platinum site that does not allow the surface passivity. All these signals totally disappear in successive anodic potential scans, except for peaks at 0.75 and 1.2 V that needs more than ten cycles to reach the usual repetitive platinum potentiodynamic profile.

On the other hand, chronoamperometric plots at 0.70 V in 0.50 M methanol + 0.5 M sulphuric acid on the pc and PS platinum is shown in Figs. 2 and 3, respectively. Methanol oxidation chronoamperometric decays were normalized with respect to the real surface area on *PS* treated platinum. The current densities were larger than those obtained with pc platinum or metal modified platinum, denoting a strong catalytic behavior towards methanol oxidation as found before [54]. The open configuration of the resulting surface depicts the possibility of having new active sites for catalytic purposes [54]. This type of surface involves new active sites towards methanol oxidation not developed by metal modifiers.

3.2. Platinum modified surfaces by a second metal: methanol bulk oxidation

3.2.1. Platinum modified by inhibiting metals: silver

The application of a potentiostatic or galvanostatic pulse is required in all electrodeposition methods; however, good results (especially at low coverages) have been obtained using the spontaneous deposition [34–38]. Large values of coverage can be reached by multiple spontaneous depositions as it has been demonstrated for ruthenium on Au(1 1 1) and for tin on pc platinum [39]. Besides ruthenium and osmium, there is lack of information about the physicochemical properties of spontaneous deposition [40]. Silver deposition has been studied by a large number of techniques [41–44], being most of them on gold and platinum in sulphate or perchlorate electrolytes. Two different stages for silver deposition on platinum were observed; one at 1.1 V responding to silver–platinum alloy electrodissolution (overlapped with the oxygen-electroadsorption at free platinum sites) and the other at 0.65 V due to the silver oxidation (from the onset of the bulk deposition process) deposited on the former surface alloy [45].

The electrochemical contour of the silver spontaneous deposition can be observed in Fig. 4 from 0.05 to 1.50 V in oxygen free sulphuric acid solution. Spontaneous deposition produces

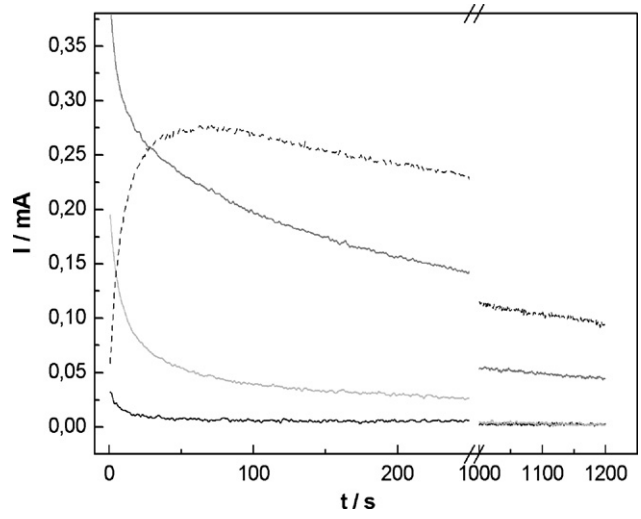

Fig. 3. Chronoamperometric plots for methanol oxidation on cathodically treated platinum (at $E = -1$ V for 5 min in acid solution) recorded at different electrode potentials in oxygen free 0.50 M methanol + 0.5 M sulphuric acid; 0.40 V (continuous line), 0.65 V (light grey line), 0.70 V (grey line), 0.775 V (dotted line).

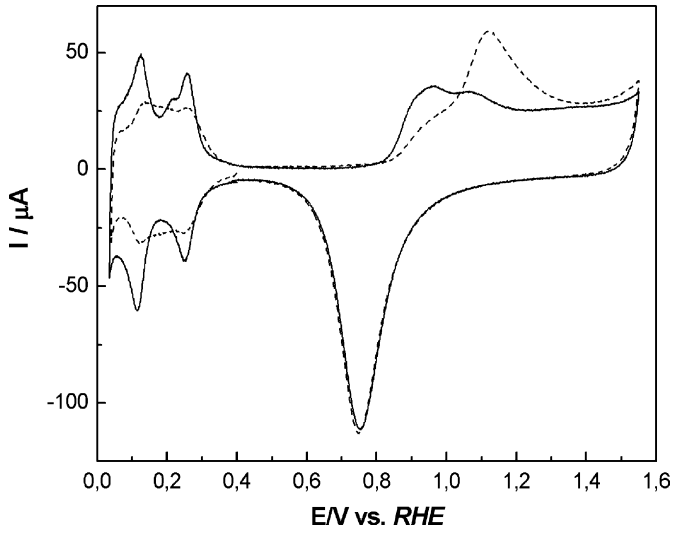

Fig. 4. Cyclic voltammetric profiles of stabilized silver spontaneous deposition (dashed line) on pc platinum run from 0.05 to 1.50 V at 0.010 V s^{-1} in oxygen free 0.5 M sulphuric acid solution at room temperature. Continuous line depicts the cyclic voltammetric profile of bare pc platinum. Silver spontaneous deposition is attained in 1 mM silver sulphate + 1 M sulphuric acid solution for t_{dep} = 60 s at room temperature.

low surface coverages (θ_{Ag} = 0.20–0.30) comparing to those observed for the electrochemical deposition (not shown here). However, higher values can be obtained after successive spontaneous depositions. On the other hand, the weakly adsorbed hydrogen peak is positively shifted from 0.12 to 0.02 V, whereas the "third anodic peak" (at 0.195 V) and the strong hydrogen adsorbate are similar populated by hydrogen ad-atoms. The main difference arising from higher coverage values of silver deposition is the appearance of a sharp peak beginning at 0.5 V.

3.2.2. Platinum modified by catalytic metals: ruthenium and osmium

Ruthenium and osmium depositions on platinum are of special interest to methanol oxidation in fuel cells. Among the different ways to deposit ruthenium or osmium on platinum [46–49], that of spontaneous deposition is attractive because of its simplicity and the fast surface concentration plateau reached after several seconds. They are very stable and normally change to stable hydroxides and oxides when the electrode potential is increased. The *ex situ* examination of the process by *STM* images on Pt(1 1 1) at the submonolayer levels shows the formation of islands [50] with maximum 0.20 ML coverage for ruthenium (at 120 s of exposure) and 0.15 ML coverage for osmium (at 60 s of exposure). Depending on the osmium coverage the island diameter varies from 2 to 5 nm [51]. The island density increases with ruthenium coverage values, but in the case of osmium there is no optimum island size [51].

To check for the voltammetric features of foreign metals oxidation on platinum, voltammetric runs were performed with upper potentials larger than 0.80 V. Fig. 5 shows the cyclic voltammetric profile of ruthenium spontaneous deposition on pc platinum when the upper potential limit is extended up to 1.50 V. As found before, ruthenium species partially inhibits the hydrogen electrosorption reaction. Fig. 5 shows the slow increase of the oxidation current near 0.6 V probably due to the formation of RuO_2 and RuO_3 surface species detected by *XPS* measurements [52]. After extending the potential towards more positive values, the partial inhibition of the oxygen electrosorption reaction is clear as a lower reduction charge density is observed in the reverse scan. Moreover, a sudden increase in the current previous to the oxygen evolution reaction is also depicted in the same figure due to co-adsorbed chloride oxidation.

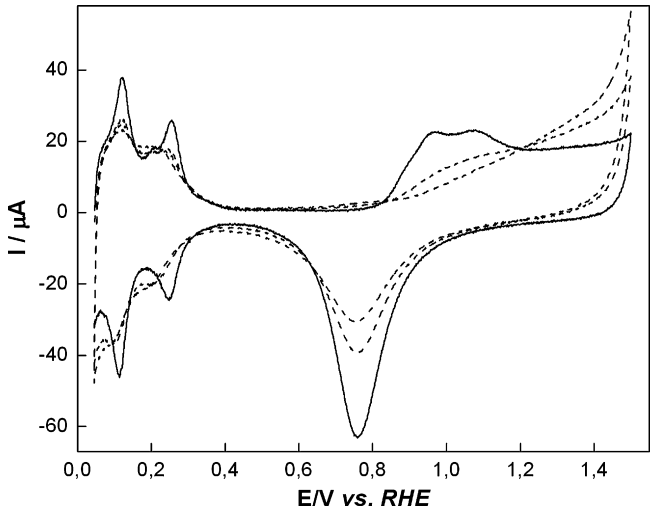

Fig. 5. Cyclic voltammetric profile of spontaneous deposition of ruthenium (dashed line) performed from 0.05 to 1.50 V at 0.1 V s^{-1} (first and sixth cycles) compared to pc platinum (continuous line) in 0.5 M sulphuric acid.

Fig. 6 shows the adsorption of osmium-containing species on pc platinum when the potential limit is extended up to 1.5 V at 0.10 V s^{-1}. In the first positive going potential scan, the inhibition of the oxygen-electrosorption is also evidenced, due to the presence of metallic osmium and osmium-oxygen containing species at a sub-monolayer level. According to results found by

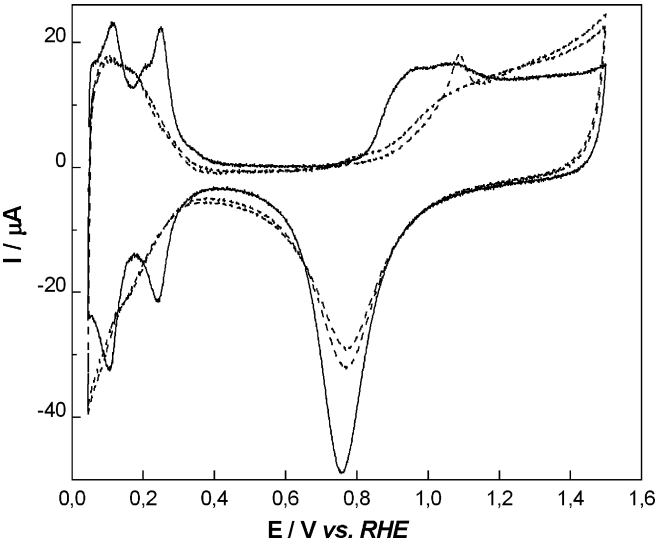

Fig. 6. Cyclic voltammetric profile of spontaneous deposition of osmium (dashed line) performed from 0.05 to 1.50 V at 0.1 V s^{-1} (two first cycles) compared to pc platinum (continuous line) in 0.5 M sulphuric acid.

XPS core-level spectra [53] and contrary to the case of ruthenium, metallic osmium can be found in the whole potential range, i.e., also up to 1.4 V. The nature of the oxidized species of osmium is OsO_2 in the entire potential region from 0.05 to 1.50 V, but with only 25% of a metallic osmium monolayer [53]. Moreover, it is also seen in Fig. 6 that the oxidation peak of osmium species is only observed in the first positive going potential scan, probably due to the dissolution of Os^{8+} ad-atoms at 1.0 V. During the second cycle the shoulder just prior to oxygen electrosorption reaction, located between 0.70 and 0.85, is better observed.

The electrochemical response of ternary platinum/ruthenium/osmium systems in the hydrogen ad-atom potential region was studied previous to methanol oxidation. The comparison of each voltammetric profiles run from 0.05 to 0.80 V at 0.10 V s^{-1} for the different surfaces shows that there are similarities between voltammetric profiles of surfaces covered by osmium containing species (not shown here). The broad pattern of the hydrogen potential region and the lack of well defined peaks for the three curves resemble that of a solely osmium deposition. It seems that osmium species governed the deposition process when it is deposited before or after ruthenium. The values of θ resulting from the calculations of the voltammetric hydrogen ad-atom region were always ca. 0.25.

We have performed the chronoamperometric curves in 0.5 M methanol + 0.5 M sulphuric acid solutions on bare platinum, platinum/silver, platinum/ruthenium/osmium, platinum/osmium and platinum/ruthenium surfaces (Fig. 7). The selected potential was 0.70 V, where oxygen-containing species (but no bulk platinum oxides) are present in all the studied surfaces. A background experiment was also performed in the absence of methanol (only with supporting electrolyte) to check for the double layer-charging component at each potential. When subtracting this current contribution, we can calculate the early stages of the methanol oxidation rate at 0.70 V.

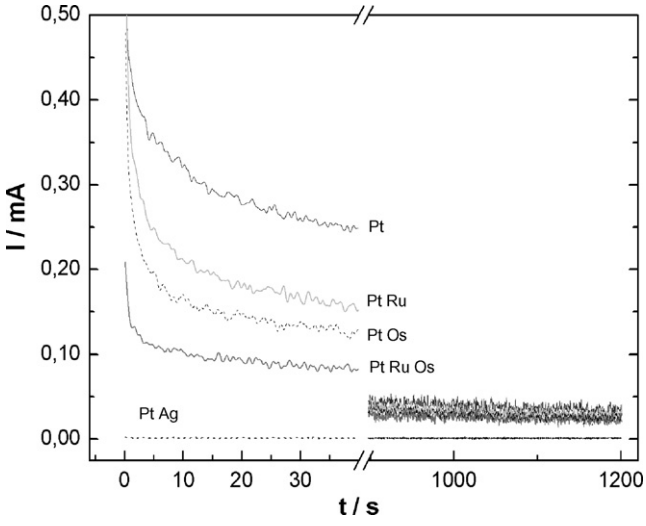

Fig. 7. Chronoamperometric plots for methanol oxidation on modified platinum (at $E = -1$ V for 5 min in acid solution) recorded at 0.70 V in oxygen free 0.50 M methanol + 0.5 M sulphuric acid; bare platinum (black continuous line), platinum/silver (dotted line), platinum/ruthenium (light grey line), platinum/osmium (dashed line), platinum/ruthenium/osmium (dark grey line).

It seems that the best catalytic effect can be attributed to bare platinum, but at very long times platinum/osmium surfaces seem to depict larger currents. The ratio between the slope of the current transient curve at zero time and the observed current at long times shows interesting results. The platinum/osmium surface exhibits the highest values of methanol oxidation rates, followed by platinum/ruthenium/osmium. The "synergetic effect" between ruthenium and osmium is evidenced in these experimental conditions.

Theoretically, methanol dissociation on ruthenium (not in the case of tin or silver) is as favourable as on pure platinum as explained above. Water dissociation on ruthenium is significantly more favourable than on platinum. This means that we have the same probability for water decomposition on both surfaces but only platinum has the ability at room temperature to adsorb methanol. The water dissociation to hydroxyl on ruthenium is slightly exothermic (−0.05 eV) in contrast to dissociation on pure platinum, which are quite endothermic (0.81 eV) [17]. Therefore, we expect that at the early stages of the process the bare platinum surface would exhibit a good performance upon methanol oxidation, but it has to decrease in comparison with the modified platinum surfaces; i.e. this is shown in Fig. 7 where at times lower than 100 s, the best catalyst seems to be platinum, while at times ca. 800 s the best performance is observed for platinum/osmium at 0.70 V as explained above.

A totally different situation is observed for methanol oxidation on bare platinum surfaces at potentials larger than 0.7 V, where instead of having a current decreasing with time we observe a current that increases with time (Fig. 2). This means that adsorbed carbon monoxide oxidation is faster than methanol decomposition reaction. The recorded current increases due to a slow increase in carbon monoxide coverage, which is rapidly oxidised. In this situation, the initial carbon monoxide oxidation reaction is fast but it slows down after some time as a result of an increased poisoning of the surface. Therefore, at potentials higher than 0.775 V, the incorporation of carbon monoxide oxidation reaction (not as poison but as a parallel reaction) is indebted, i.e. the potential range for our model is narrower due to this problem. Thus, an improved parallel mechanism together with an analytical solution of the differential equation is in advance.

4. Methanol oxidation reaction mechanism

In the platinum/aqueous acid solution interface and under 0.4 V the hydrogen adsorption/desorption reversible reaction takes place:

$$H^+ + e^- \leftrightarrow H_{ads} \quad (I)$$

On the other hand, adsorption of water in the double layer with a further discharge from 0.7 V occurs in acid solution on a bare platinum surface:

$$H_2O + Pt \leftrightarrow Pt\text{–}H_2O_{ads} \quad (II)$$

$$Pt\text{–}H_2O_{ads} \leftrightarrow Pt\text{–}OH_{ads} + H^+ + e^- \quad (III)$$

The interaction of these species with platinum is rather weak, except at potentials lower than 0.10 V where methanol adsorbed species are not able to displace hydrogen adsorbates and at potentials larger than 0.90 V methanol adsorption strongly competes with oxygen-containing species on platinum.

The first interaction of methanol with platinum can be characterised by the subsequent losses of hydrogen from carbon atom, occupying various platinum adjacent sites. The number of these sites depends on the crystal orientation of the substrate, methanol concentration and pH.

$$CH_3OH + 2Pt \rightarrow Pt\text{–}CH_2\text{–}OH_{ads} + Pt\text{–}H_{ads} \quad (IV)$$

$$Pt\text{–}CH_2\text{–}OH_{ads} + 2Pt \rightarrow Pt_2\text{–}CH\text{–}OH_{ads} + Pt\text{–}H_{ads} \quad (V)$$

$$Pt_2{=}CH\text{–}OH_{ads} + 2Pt \rightarrow Pt_3{\equiv}C\text{–}OH_{ads} + Pt\text{–}H_{ads} \quad (VI)$$

However, it has been shown that all of them are converted to Pt-CO (or Pt-COH) and some Pt-H depending on the involved potential range:

$$Pt_3{\equiv}C\text{–}OH_{ads} \rightarrow Pt{=}CO_{ads} + Pt\text{–}H_{ads} \quad (VII)$$

The species Pt-COH and/or Pt-CO can react with surface hydroxyl species (III) when they are located at a nearby position. Finally, the products are oxidatively desorbed from the surface making platinum available for further acts of reaction.

$$Pt_3{\equiv}C\text{–}OH_{ads} + Pt\text{–}OH_{ads} \rightarrow Pt\text{–}CO_{ads} + H_2O_{ads} + 3Pt \quad (VIII)$$

$$Pt\text{–}CO_{ads} + Pt\text{–}OH_{ads} \rightarrow Pt\text{–}COOH_{ads} + Pt \quad (IX)$$

$$Pt\text{–}COOH_{ads} + Pt\text{–}OH_{ads} \rightarrow CO_2 + H_2O + 2Pt \quad (X)$$

A theoretical study has been performed using the extensive density-functional theory for the analysis of the adsorption behaviour of carbon monoxide on platinum and mixed Pt–M clusters (M = ruthenium, tin, germanium) [17]. This study examined the effect of M alloying atoms in water dissociation, where the presence of M atoms decreases the PtM–CO bond strength. The activation energy for this process is smaller on ruthenium than on platinum. On the simulated cluster alloys of $(Pt_3)(Ru_2Pt_5)$ water dissociation is also more endothermic and has slightly higher activation energy than on pure platinum [17]. On the other hand, methanol dissociation to COads occurs easily for pure platinum. They found that ruthenium in platinum/ruthenium alloys promotes methanol dissociation and the formation of hydroxyl adsorbates from adsorbed water. Their conclusion establishes that an alloy with a relatively high ruthenium/platinum ratio should be beneficial for methanol oxidation.

Some earlier paper [55] assumed that methanol oxidation does not proceed through a series of consecutive reactions, but through a parallel path mechanism, forming a poisoning species through it. Thus, carbon dioxide may be formed by the direct oxidation of methanol or by the oxidation of adsorbed carbon monoxide at higher electrode potentials [13,28,56]. Using a chronoamperometric analysis of methanol oxidation on Pt(1 1 1), Pt(1 1 0), and Pt(1 0 0), Franaszczuk et al. [12] modelled the poisoning effect, with only the direct methanol oxidation and the formation of COads through a direct reaction pathway. The expression for the methanol-related oxidation current recorded in these transients' contained four fitting parameters. However, it seems to be quite empirical because they assumed a rate constant of the site blocking process (decomposition of methanol) with a single number of surface sites to convert methanol into carbon monoxide.

Lu et al. [57] modified the former model to fit the experiments for methanol oxidation on pc platinum. They added an exponential current decay to the expression of the current transients to account for the fast observed current decrease at times lower than 40 ms. This was ascribed to species formed during the initial oxidation, other than adsorbed carbon monoxide, reporting a noticeable improvement in the fit. Vielstich and Xia [58] establish that the use of the initial current density in chronoamperometric data as a fitting parameter is somewhat confusing. They also found that methanol does not oxidise completely to carbon dioxide because of carbon monoxide blockage, so a more complicated interpretation of the parameter has to be sketched.

Stuve and co-workers [28] proposed the only model that incorporates carbon monoxide oxidation along with methanol direct oxidation and decomposition reactions. However, rather than using directly the chronoamperometric data, they chose to model the relationship between the charge under the transients and the charge obtained after stripping the electrode from adsorbed species in a different cell. The results clearly showed that at short times (<30 ms) only partial oxidation products and virtually no carbon dioxide are formed. At times longer than 5 s, carbon dioxide production is greatly favoured over residue formation. They also concluded that for methanol oxidation on Pt(1 1 1) electrodes a serial reaction path, involving adsorbed intermediates, is inadequate to describe the observed rate of carbon dioxide formation. Baltruschat et al. [59] proposed a parallel pathway mechanism in which carbon dioxide could be formed through the oxidation of adsorbed carbon monoxide or the oxidation of intermediate dissolvable species such as formic acid and formaldehyde.

5. On the proposed model

According to the above results by other authors, it seems that the parallel reaction pathway for methanol oxidation works for low plane and stepped platinum single crystals [60]. However, we propose for pc platinum a direct series oxidation mechanism setting the current produced in the direct path without making any assumptions regarding the nature of the reaction steps, the amount of electrons produced per methanol molecule, or the formed products. In other words, our model is simple and without any improvements over previous models, but with a whole kinetic treatment for the overall series mechanism. Nevertheless, many authors have shown [15,36] (for example) that the contribution of the direct pathway can be considerable on carbon monoxide-covered electrode surfaces and that the direct pathway has to be the main process of the mechanism.

The following four-step reaction pathway in a series mechanism is proposed neglecting the intermediates of methanol

dehydrogenation in the 0.4–0.8 V versus RHE potential ranges and considering the surface recombination of COads and OHads as the determining step.

$$CH_3OH + Pt \overset{k_{ox,1}k_{red,1}}{\longleftrightarrow} Pt - CH_{3-x}OH_{ads} + xH^+ + xe^- \quad (XI)$$

$$Pt - CH_{3-x}OH_{ads} \overset{k_{ox,2}k_{red,2}}{\longleftrightarrow} Pt - CO_{ads} + (4-x)H^+ + (4-x)e^- \quad (XII)$$

$$Pt + H_2O \overset{k_{ox,3}k_{red,3}}{\longleftrightarrow} Pt - OH_{ads} + H^+ + e^- \quad (XIII)$$

$$Pt - CO_{ads} + Pt - OH_{ads} \overset{k_{ox,4}}{\longrightarrow} CO_2 + H^+ + e^- + 2Pt \quad (XIV)$$

$k_{ox,i}$ and $k_{red,i}$ being the electrochemical rate constants for each oxidation and reduction pathways, respectively. The rate determining step, $k_{ox,4}$, is of second order but since θ is defined dimensionless, it is expressed in [s^{-1}].

The following surface condition is applied:

$$\theta_{CO} + \theta_{OH} = 1 \quad (2a)$$

which is equivalent to:

$$\frac{\partial\theta_{CO}}{\partial t} = -\frac{\partial\theta_{OH}}{\partial t} \quad (2b)$$

In our model it is assumed that:

(1) There is no distinction between each adsorbed carbonaceous species in the series mechanism.
(2) All the oxygen-containing species are equivalent to hydroxyl adsorbates.
(3) The reaction occurs under the Eqs. (XI)–(XIV) without any presence of platinum oxide precursors or hydrogen adsorbates.
(4) Bulk methanol and proton concentrations are considered as constants.

5.1. The kinetic law of the series mechanism in methanol electrooxidation

In the case of an electrocatalytic reaction; the current density ($\vec{j}$) can be evaluated through the change in the surface coverage by carbon monoxide adsorbates (θ)

$$\vec{j}(t) = \sigma\frac{d\theta}{dt} = \sigma\frac{d(\Gamma/\Gamma_{sat})}{dt} = \frac{F}{N_A}\frac{d\Gamma}{dt} = F\frac{dc}{dt} \quad (3a)$$

c being the surface concentration in [mol cm^{-2}], F the Faraday constant [C mol^{-1}], σ the maximum surface charge density in [C cm^{-2}], Γ and Γ_{sat} the surface excess at any time and at under saturation conditions in [molecules cm^{-2}] with $\Gamma_{sat} = N_A\sigma/F$, N_A being the Avogadroĭs number.

The current density for a Faradaic process is given by the electrochemical rate of reaction ($\vec{v}$):

$$\vec{j}(t) = nF\vec{v}(t) = nF\vec{k}\prod_i c^{p_i} \quad (3b)$$

n being the number of electrons, $k \rightarrow$ the potential dependent rate constant and p_i the reaction order for bulk and surface concentrations of reactants.

Considering Eqs. (3a) and (3b) and on the base of our model assumptions, we have the following expression of the kinetic law in the series mechanism:

$$\sigma\frac{d\theta}{dt} - F[(4-x)k_{ox,2} - xk_{red,1}(H^+)^x - (4-x)k_{red,2}(H^+)^{4-x} + k_{red,3}(H^+)]\theta + Fk_{ox,4}\theta^2 - (4-x)Fk_{ox,1}(CH_3OH) + Fk_{ox,3} = 0 \quad (4)$$

An interesting prediction that follows from Eq. (4) is that the shape of the current transient strongly depends on the relative numerical values of k_{ox} and k_{red}. Therefore, by condensing the terms we will have:

$$\frac{d\theta}{dt} + \theta K + \theta^2 L + M = 0 \quad (5)$$

with

$$K \equiv \frac{F}{\sigma}[(4-x)k_{red,2}(H^+)^{4-x} - (4-x)k_{ox,2} + xk_{red,1}(H^+)^x - k_{red,3}(H^+)] \quad (6a)$$

$$L \equiv \frac{Fk_{ox,4}}{\sigma} \quad (6b)$$

$$M \equiv \frac{F}{\sigma}[k_{ox,3} - (4-x)k_{ox,1}(CH_3OH)] \quad (6c)$$

According to (5) and (6) the dimensions of K, L and M are [$cm^2\ mol^{-1}\ s^{-1}$], whereas the dimensions of k_{ox} and k_{red} have to be [s^{-1}]. If the surface coverage were defined as an absolute coverage (Γ in [mol cm^{-2}]) the dimensions of k_i would be dependent of the reaction order.

Expression (5) is the quadratic Bernoulli equation, known as Ricatti equation, of non-linear differential equations with potential dependent coefficients [61]. Since the quadratic integration of this equation is not analytically simple, the search of the solution cannot be reduced to a finite number of successive integrations. In Appendix A we have a brief summary of what we can do to solve the Ricatti's expression with the substitution Theorem.

We can change to a new variable in Eq. (5) of the form:

$$\theta \equiv \frac{h'N_A}{hL\Gamma_{sat}} \quad (7)$$

Then, Ricatti's expression is reduced to a second order linear equation, which after reordering will be:

$$h'' + Kh' + \frac{\Gamma_{sat}LM}{N_A}h = 0 \quad (8)$$

The coefficients of the equation contain the potential dependent rate constants of the chronoamperometric experiments. Then, we can work with the constant coefficient characteristic equation.

$$r^2 + Kr + \frac{\Gamma_{sat}LM}{N_A} = 0 \quad (9)$$

which has the following solution:

$$r_{1,2} = -\frac{K}{2} \pm \sqrt{\left(\frac{K}{2}\right)^2 - \frac{\Gamma_{sat} L M}{N_A}} \quad (10)$$

The general solution of the differential equation will be:

$$h = C_1 \exp(r_1 t) + C_2 \exp(r_2 t) \quad (11)$$

Taking the first derivative

$$h' = C_1 r_1 \exp(r_1 t) + C_2 r_2 \exp(r_2 t) \quad (12)$$

and substituting it by Eq. (7), we obtain the value of θ

$$\theta = \frac{h' N_A}{h L \Gamma_{sat}} = \frac{N_A (C_1 r_1 \exp(r_1 t) + C_2 r_2 \exp(r_2 t))}{\Gamma_{sat} L (C_1 \exp(r_1 t) + C_2 \exp(r_2 t))} \quad (13)$$

and since $L \equiv F k_{ox,4}/\sigma$ the current density expression will be:

$$j(t) = \sigma \frac{d\theta}{dt} = \frac{N_A \sigma^2}{\Gamma_{sat} F k_{ox,4}} \frac{C_1 C_2 (r_1 - r_2)^2 \exp((r_1 + r_2)t)}{(C_1 \exp(r_1 t) + C_2 \exp(r_2 t))^2}$$
$$= \Delta \frac{\exp((r_1 + r_2)t)}{(C_1 \exp(r_1 t) + C_2 \exp(r_2 t))^2} \quad (14a)$$

$$\text{with} \quad \Delta \equiv \frac{\sigma C_1 C_2 (r_1 - r_2)^2}{k_{ox,4}} \quad \text{since } \Gamma_{sat} = N_A \sigma / F \quad (14b)$$

This is the expression of the chronoamperometric current based on the series oxidation reaction model. Table 1 shows the values of each parameter for the different platinum modified electrodes.

Table 1
Parameters for Eqs. (14a) and (14b) for chronoamperometric data at 0.70 V at different platinum and metal modified surfaces; ruthenium, osmium, ruthenium:osmium and silver in 0.50 M methanol + 0.5 M sulphuric acid

	Δ (A cm^{-2})	r_1 (s^{-1})	r_2 (s^{-1})	C_1	C_2
Pt	3.016×10^{-6}	0.06578	0.0527	0.12197	−0.0299
Pt PS	5.606×10^{-7}	0.06977	0.05657	0.03254	−0.00816
Pt Ru	2.346×10^{-6}	0.06668	0.0348	0.13743	−0.04842
Pt Os	1.533×10^{-6}	0.06922	0.0618	0.16037	−0.04111
Pt Ru Os	2.085×10^{-6}	0.06958	0.0262	0.13758	−0.04723
Pt Ag	2.958×10^{-3}	0.11816	0.0132	0.21208	−0.02542

The values of the fitting parameters at different electrode potentials were calculated for pc and PS platinum and plotted in Figs. 8 and 9. The values of the pre-exponential factor, Δ, includes the exchange current density of the reaction on both pc and PS platinum. It increases with the electrode potential, showing that the reaction requires the presence of hydroxyl-species on the surface to be activated from 0.6 V. On the other hand, the values of C_1 changes with the potential in an opposite way as those of C_2 as a consequence of the resulting sign. C_1 is positive and has the lowest value at the largest studied electrode potentials, whereas C_2 exhibits its largest values (less negative) in the same region. This means that C_1 is involved in the methanol adsorption process, which is large in the hydrogen adsorption region (at potential higher than 0.10 V versus RHE).

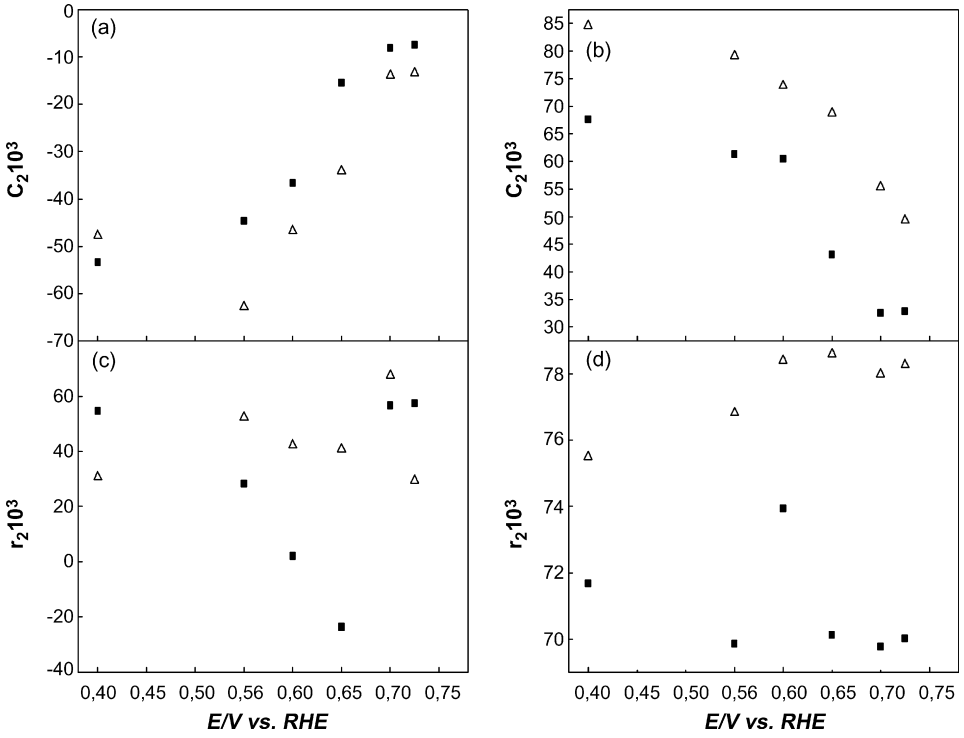

Fig. 8. (a–d) Chronoamperometric fitting parameters: C_2, C_1, r_2 and r_1 for methanol oxidation on cathodically treated (open triangles) and bare (full squares) platinum. The cathodically treated platinum was prepared as explained in the text. The chronoamperometric curves were recorded at different potentials in oxygen free 0.50 M methanol + 0.5 M sulphuric acid.

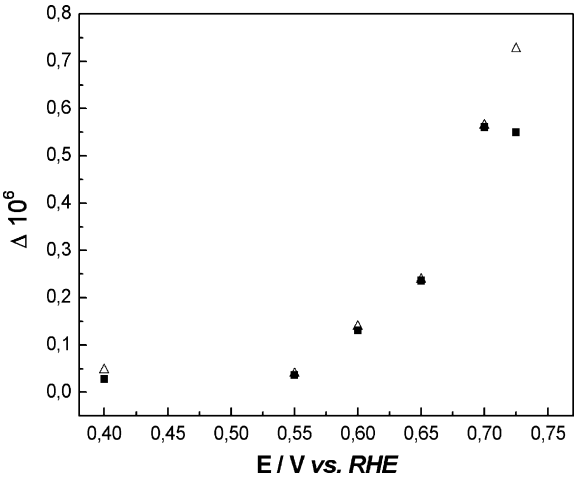

Fig. 9. Chronoamperometric fitting parameter Δ for methanol oxidation on cathodically treated (open triangles) and bare (full squares) platinum. The cathodically treated platinum was prepared as explained in the text.

C_2 is concerned on the methanol oxidation process because of its potential dependence. Similar tendencies are observed for the PS platinum surfaces but with much larger values for C_1 and lower values for C_2.

However, one of the most important features in the current density expression is the shape of the current decay. This response can be envisaged through the values of r_1 and r_2. In the case of r_2 the values softly decreases until 0.65 V, showing that this parameter is well associated to methanol oxidation. The values on PS platinum are larger until this potential value, but later are practically the same to those of pc platinum. On the other hand, the situation is not so clear for r_1 since the increase with potential seems to be saturated up to 0.60 V, coincidently with the minimum adsorption of methanol (competition with oxygen from the water discharge). The values are much higher for the PS surfaces at all potentials, showing that the current exponential decay is faster on pc platinum.

A comparison between the fitting results in the case of methanol oxidation shows good correlation at times lower than 200 s, however at larger times the problem of overestimation appeared (not shown). One of the main reasons probably arises from the lack of correlation between our model and the carbon monoxide path in parallel.

The complete expression of the current can be analysed through its slope at zero time, the current value at the asymptotically infinite time and the expression of the time dependence of the surface coverage by methanol adsorbates.

5.1.1. The slope of the current density at zero time for methanol electrooxidation

The slope can be evaluated from the current versus time first derivate:

$$\frac{\mathrm{d}j(t)}{\mathrm{d}t} = \left(\frac{\sigma C_1 C_2 (r_1 - r_2)^2}{k_{\mathrm{ox},4}}\right) \frac{(r_1 + r_2)(C_1 \exp(r_1 t) + C_2 \exp(r_2 t)) \exp((r_1 + r_2)t) - 2\exp((r_1 + r_2)t)}{(C_1 \exp(r_1 t) + C_2 \exp(r_2 t))^3} \tag{15}$$

By taking the value at zero time:

$$\left.\frac{\mathrm{d}j(t)}{\mathrm{d}t}\right|_{t=0} = \left(\frac{\sigma C_1 C_2 (r_1 - r_2)^2}{k_{\mathrm{ox},4}(C_1 + C_2)^2}\right) \times \left[(r_1 + r_2) - \frac{2(C_1 r_1 + C_2 r_2)}{(C_1 + C_2)}\right] \tag{16}$$

The sign of the slope seems to be always negative in the base of this model, since the results of the fitting from Table 1 show that $(r_1 + r_2) \approx 10(C_1 r_1 + C_2 r_2)$ except for the only two exceptions of pc platinum with $5.5\,10^{-5}\,\sigma/k_{\mathrm{ox},4}$ and PS platinum with $6.9\,10^{-6}\,\sigma/k_{\mathrm{ox},4}$. These exceptions are more notorious at higher potentials as it can be seen in Fig. 3.

According to the chronoamperometric data by Housmans and Koper [60] the transients recorded on Pt(1 1 1) showed an initial current increase, which may be explained by the carbon monoxide oxidation being faster than the methanol decomposition. This low decomposition rate is probably the result of a sufficiently low defect density on the metal and the low methanol concentration used in their experiments. They fit the chronoamperometric data with a mathematical model, which includes methanol decomposition, carbon monoxide oxidation and direct methanol oxidation. The model indeed predicts that when the carbon monoxide oxidation rate is faster than the decomposition rate, a rising current transient can be expected, as we see for pure pc platinum. In this case it seems to be better to mimic methanol oxidation reaction with a parallel carbon monoxide and carbon dioxide mechanism.

The analysis of the chronoamperometric parameters of Table 1 for metal-modified platinum surfaces shows that the most dramatic initial current versus time slope occurs on the ternary surface compound of ruthenium/osmium ($-1.3 \times 10^{-3}\,\sigma/k_{\mathrm{ox},4}$). On the other hand, the lowest initial current versus time slope is observed for the platinum/silver surface compound with $-7.4 \times 10^{-4}\,\sigma/k_{\mathrm{ox},4}$. Besides, on platinum/ruthenium and platinum/osmium the slopes are $-8.1 \times 10^{-4}\,\sigma/k_{\mathrm{ox},4}$ and $-2.4 \times 10^{-4}\,\sigma/k_{\mathrm{ox},4}$, respectively.

The analysis of the slope of the current versus time at $t = 0$ involves the electrochemical rate constant of the determining step ($k_{\mathrm{ox},4}$) or said in other words the co-adsorbate catalytic oxidation, i.e. the oxidation of COads with OHads. Thus, depending on the value of $k_{\mathrm{ox},4}$ each slope can change its order of magnitude. In the case of having a large L, the values of the slopes will decrease. This means that the current observed for platinum denotes a low residential time for adsorbed carbon monoxide. On the other hand, a totally different situation arises for small L values; thus, the surfaces will denote a large residential time for COads, i.e. a slow oxidation of the adsorbate.

5.1.2. The current density value at the asymptotically infinite time for methanol oxidation

It is really important to evaluate the time at which the current transient reach the steady state, since it is a characteristic of the electrocatalyst. This is achieved considering in Eq. (15) the following reorder of terms by multiplying and dividing by $\exp(-(r_1+r_2)t)$:

$$\frac{dj(t)}{dt} = \left(\frac{\sigma C_1 C_2 (r_1-r_2)^2 (r_1+r_2)\exp((r_1+r_2)t)}{k_{ox,4}(C_1\exp(r_1t)+C_2\exp(r_2t))^3}\right) \times (C_1\exp(r_1t)+C_2\exp(r_2t)-2) \quad (17)$$

There is no change in

$$\frac{dj(t)}{dt} \quad (18a)$$

when either

$$C_1\exp(r_1t)+C_2\exp(r_2t)-2=0 \quad (18b)$$

and/or $r_1 = r_2$

(1) In the first case the comparison between both exponential terms can be reduced since they are both of the same shape but with a different expansion with time. Thus, they can be simplified to a single exponential contribution. However, looking at Table 1 we can say that $r_1 = r_2 + a$, $C_1 = -(C_2 + b)$, a and b being experimental parameters dependent on the type of platinum surface. Thus, Eq. (18a) renders for the steady state time, t_{ss}:

$$C_1\exp(r_1t_{ss})+C_2\exp(r_2t_{ss})-2 = -(C_2+b)\exp((r_2+a)t_{ss})+C_2\exp(r_2t_{ss})-2=0 \quad (19)$$

or

$$[C_2 + C_1\exp((r_1-r_2)t_{ss})]\exp(r_2t_{ss}) = 2 \quad (20)$$

The situation implies large times so we can say $C_2 \ll (C_2 + b)\exp((r_1 - r_2)t_{ss})$, therefore:

$$t_{SS} = \frac{\ln(2/C_1)}{r_1} + \text{cte.} \quad (21)$$

The relaxation time (at which the steady state is reached) indicates how fast the coverage of the intermediate will relax back to an equilibrium value after perturbation. Table 2 shows the value proportional to t_{ss} obtained from Eq. (21). It is possible to conclude that for PS treated platinum the t_{ss} value is slightly larger than for pc platinum and more properly is the largest of all, i.e. ca. 59 + cte. On the other hand, the value of t_{ss} for platinum/ruthenium surfaces is near that of pc platinum, whereas it decreases for osmium and ruthenium/osmium surfaces. The steady state current for platinum/silver is reached at the lowest t_{ss} values, showing again that the surface exhibits inhibitory characteristics (t_{ss} ca. 19 + cte).

(2) The other condition (18b) $r_1 = r_2$ implies

$$r_2 = r_1 \to -\frac{K}{2} - \sqrt{\left(\frac{K}{2}\right)^2 - \frac{\Gamma_{sat}LM}{N_A}} = -\frac{K}{2} + \sqrt{\left(\frac{K}{2}\right)^2 - \frac{\Gamma_{sat}LM}{N_A}} \quad (22)$$

This situation only accounts when:

$$\left(\frac{K}{2}\right)^2 = \frac{\Gamma_{sat}LM}{N_A} \quad (23)$$

that is,

$$N_A F(xk_{red,1}(H^+)^x + (4-x)k_{red,2}(H^+)^{4-x} - k_{red,3}(H^+) - (4-x)k_{ox,2})^2 = -4F^2\Gamma_{sat}(x(CH_3OH)k_{ox,4}k_{ox,1} - k_{ox,4}k_{ox,3}) \quad (24)$$

However, this is a complex combination of electrochemical rate constants. It would be better to analyse the difference between each r_1 and r_2. On one hand, we can obtain the values of K, L and M from the difference between r_1 and r_2:

$$\left(\frac{r_1-r_2}{2}\right)^2 = \left(\frac{K}{2}\right)^2 - \frac{\Gamma_{sat}LM}{N_A} \quad (25)$$

On the other hand, from the addition of r_1 and r_2, we have the value of K (Table 2)

$$K = -(r_1+r_2) \quad (26)$$

Considering that Eq. (26) renders negative values of K and since K is given by (6a) it is likely that the contribution of $k_{ox,2}$ and $k_{red,3}$ has to be larger than $k_{red,1}$ and $k_{red,2}$. By substitution of K into (25) we can obtain the product LM. The values of L are given above from the slope of the current transient at zero time.

$$\left(\frac{r_1-r_2}{2}\right)^2 = \left(\frac{-(r_1+r_2)}{2}\right)^2 - \frac{\Gamma_{sat}LM}{N_A} \quad (27)$$

Then, by simplifying the expression we can obtain

$$\frac{\Gamma_{sat}LM}{N_A} = \left(\frac{-(r_1+r_2)}{2}\right)^2 - \left(\frac{r_1-r_2}{2}\right)^2 \quad (28)$$

or

$$\frac{\Gamma_{sat}LM}{N_A} = \frac{-(r_1^2+r_2^2)}{2} \quad (29)$$

The term $r_2^1 + r_2^2$ calculated from Table 1 is always positive and considering Eqs. (29) and (6) the product LM will be negative:

$$\sigma LM = -F^2[(4-x)(CH_3OH)k_{ox,4}k_{ox,1} - k_{ox,4}k_{ox,3}] \quad (30)$$

Since LM is negative, Eq. (30) indicates that $k_{ox,3}$ is smaller than $(CH_3OH)k_{ox,1}$. However, we can separately obtain L from

Table 2
Parameters K, L, M, $k_{ox,4}$, t_{ss}, $j_{t=0}$ and $dj/dt_{t=0}$ from chronoamperometric data at 0.70 V at different platinum and metal modified surfaces in 0.50 M methanol + 0.5 M sulphuric acid using data of Table 1

	$j_{t=0}$ (A cm^{-2})	$dj/dt_{t=0}$ (A cm^{-2} s^{-1})	K (cm^2 mol^{-1} s^{-1})	LM (cm^4 mol^{-2} s^{-2})	L/F (C^{-1} cm^2 s^{-1})	$k_{ox,4}$ (s^{-1})	$M\sigma$ (A mol^{-1})	t_{ss} (s) − cte
Pt	5.90×10^{-4}	7.68×10^{-6}	−0.11848	−0.00155	0.2068	5×10^{-5}	−0.00749	42.52
Pt PS	1.00×10^{-3}	2.08×10^{-5}	−0.12634	−0.00167	0.0824	2×10^{-5}	−0.00749	59.05
Pt Ru	6.62×10^{-4}	-1.97×10^{-5}	−0.10148	−0.00324	2.888	7×10^{-4}	−0.00112	40.16
Pt Os	2.23×10^{-4}	-1.35×10^{-6}	−0.13102	-9.722×10^{-4}	0.563	1×10^{-4}	−0.00173	36.46
Pt Ru Os	5.27×10^{-4}	-2.26×10^{-5}	−0.09578	−0.00415	5.861	1×10^{-3}	-7.0891×10^{-4}	38.47
Pt Ag	2.24×10^{-6}	-1.13×10^{-2}	−0.13136	−0.01379	0.02	5×10^{-6}	−0.68938	18.99

the initial current versus time slope (Eq. (16)),

$$L = \left(\frac{FC_1C_2(r_1 - r_2)^2}{(C_1 + C_2)^2 (\mathrm{d}j(t)/\mathrm{d}t)|_{t=0}} \right) \times \left[(r_1 + r_2) - \frac{2(C_1 r_1 + C_2 r_2)}{(C_1 + C_2)} \right] \quad (31a)$$

or in a simpler way from Eq. (14b)

$$L = \frac{FC_1C_2(r_1 - r_2)^2}{\Delta} \quad (31b)$$

Summing up, it is possible to obtain the values of L, M and K, which are depicted in Table 2, calculated from Eqs. (26), (29) and (31b). The most interesting parameter is L since it simply involves the value of $k_{ox,4}$. The largest value is observed for platinum/ruthenium/osmium surface ($L = 5.861F$), so since $L \equiv Fk_{ox,4}/\sigma$ then, $k_{ox,4} = 5.861\sigma$. Besides $\sigma = 2.4 \times 10^{-4}$ C cm^{-2} [60], thus, $k_{ox,4} = 0.0014$ mol^{-1} cm^2 s^{-1}.

Table 2 also shows the values of $k_{ox,4}$ for rest of the surfaces. At this point, it is important to remark that the values found for this oxidation rate constant by other authors [60] lie within the range of 10^{-3} to10^{-1} s^{-1}, considering it as a first-order reaction constant. This situation can be also envisaged from Fig. 7 (dark grey lines) for times larger than 900 s, where the chronoamperometric plot exhibits larger currents on this surface. Surprisingly, the value of L for PS platinum is almost three-fold lower than pc platinum. The situation is quite similar for platinum/ruthenium. This means that this type of surfaces are able to react better at starting times but later gets more poisoned than the original pc platinum. The situation for platinum/silver is the worst as expected.

The values of K for the six types of platinum surfaces are nearly the same (the lowest for platinum/silver). The parameter contains the first back reductive methanol adsorbate, the back formation of COads subtracted the back formation of OHads and the decomposition of the first partially dehydrogenated methanol conversion to COads. The sign on all surfaces show that the two latter's are the largest on all the studied platinum surfaces. This means that both processes are not very distinct on each modified platinum surfaces and also not rate determining.

On the other hand, the value of M involves the formation of OHads species minus the first oxidative dissociation of methanol. In all surfaces the sign is negative showing that the formation of OHads is not very fast. This is an important comparison since the problem of OHads formation is later determining the oxidation of COads. Thus, it is likely that the electrochemical rate for the first oxidation stage would be slower than expected, however it is not rate determining as it was supposed in our model. Some interesting features have to be pointed out, $M\sigma = -0.0075$ for both pc and PS platinum. This means that both electrochemical reactions: $k_{ox,1}$ and $k_{ox,3}$ does not change with the cathodisation procedure, i.e. the number of active sites for both methanol and OH species are the same. However, in the case of platinum/silver $M\sigma = -0.689$ and is the largest of all. This means that the formation of OHads and CH_{3-x}OHads are not the fastest of all, but the methanol oxidation reaction tends to be limited there, or in its COads stable species. Between ruthenium and osmium, it seems that the formation of OHads is slower on platinum/osmium and maybe also the formation of the first adsorbed species (CH_{3-x}OHads).

Another interesting correlation is the potential dependence of K, L/F and $M\sigma$ calculated from current versus time fitting parameters: C_2, C_1, r_2 and r_1 as above. The results for methanol oxidation on pc and PS platinum surfaces are qualitatively similar, so we are going to explain the results only for methanol oxidation on pc platinum. The values of K increase exponentially with the electrode potential (not shown) as expected for the decomposition of the first partially dehydrogenated methanol conversion to COads. Though, from 0.65 V it sharply falls down to the initial values denoting the influence of the OHads back formation. The same situation is observed for L/F, since after its maximum at 0.55 V it rapidly decreases attaining the saturation at $L = 0.08F$ from 0.7 V. This means that the electrochemical rate constant of the determining step reaches its optimum value at 0.55 V. On the other hand, $M\sigma$ values are nearly constant (between −4 and -5×10^{-5}) for potentials between 0.4 and 0.65 V, however from 0.7 V it sharply decreases to ca. −0.022. At these higher potentials $M\sigma$ is still negative indicating that the formation of OHads is not very fast comparing to methanol dissociation.

5.1.3. The time dependence surface coverage by methanol adsorbates for methanol oxidation (integration of the chronoamperometric curve)

On the other hand, by integrating the time dependent current density we can obtain the surface coverage by methanol adsorbates. Thus, from Eq. (14a):

$$\frac{\mathrm{d}\theta}{\mathrm{d}t} = \frac{N_A\sigma}{\Gamma_{sat}Fk_{ox,4}} \frac{C_1C_2(r_1 - r_2)^2 \exp((r_1 + r_2)t)}{(C_1 \exp(r_1 t) + C_2 \exp(r_2 t))^2} \quad (32)$$

$$\int_{\theta_i}^{\theta} \mathrm{d}\theta = \frac{C_1 C_2 (r_1 - r_2)^2}{k_{ox,4}} \int_0^t \frac{\exp\left((r_1 + r_2)\, t\right)}{(C_1 \exp(r_1 t) + C_2 \exp(r_2 t))^2} \mathrm{d}t \tag{33}$$

or we can factorise the exponential terms to reduce their exponential order:

$$\int_{\theta_i}^{\theta} \mathrm{d}\theta = -\frac{C_1 C_2 (r_1 - r_2)^2}{k_{\mathrm{ox},4}} \int_0^t \frac{\exp(r_1 t)}{(C_2 + C_1 \exp(r_1 - r_2) t)^2} \mathrm{d}t \tag{34}$$

By defining

$$\theta_{\mathrm{o}} \equiv \frac{C_1 C_2 (r_1 - r_2)^2}{k_{\mathrm{ox},4}} \tag{35}$$

we can obtain

$$\theta = \theta_i - \theta_{\mathrm{o}} \int_0^t \frac{\exp(r_1 t)}{(C_2 + C_1 \exp(r_1 - r_2) t)^2} \mathrm{d}t \tag{36}$$

θ_i being the initial surface coverage. Then, after multiplying and dividing by $\exp(r_1 - r_2)t$ and $\exp{-}(r_1 + r_2)t$

$$\theta = \theta_i - \theta_{\mathrm{o}} \int_0^t \frac{\exp(r_1 - r_2) t}{(C_1 + C_2 \exp(r_1 - r_2) t)^2} \mathrm{d}t \tag{37}$$

We can use the substitution Theorem for integration as in Appendix B to obtain the time dependence of θ

$$\theta = \theta_i - \frac{C_1 (r_1 - r_2)}{k_{\mathrm{ox},4}} \left[\frac{1}{(C_1 + C_2)} - \frac{1}{(C_1 + C_2 \exp(r_1 - r_2) t)} \right] \tag{38}$$

The surface coverage at the beginning of the current transient will be as expected:

$$\lim |_{t \to 0} \theta = \theta_i \tag{39}$$

and the value of θ at steady state ($t \to \infty$, θ_{ss}) is:

$$\lim |_{t \to \infty} \theta = \theta_{\mathrm{ss}} = \theta_i - \frac{C_1 (r_1 - r_2)}{k_{\mathrm{ox},4} (C_1 + C_2)} \tag{40}$$

We can compare this magnitude defined as $\Delta\theta = \theta_{\mathrm{ss}} - \theta_{t-0}$ in Table 3 using data of Table 1 taken for bulk methanol oxidation at 0.70 V on the different catalysts. Since the change in θ strongly depends on $k_{\mathrm{ox},4}$ we have to take into account that their values from Table 2 to calculate $\Delta\theta$. The largest of $\Delta\theta$ is observed for platinum/silver surfaces, meaning that θ_{ss} is very different to θ_{t-0}. This does not mean imply large kinetics but a strong poisoning effect, demonstrated by the value of the stationary current at 1800 s, I_{ss}. However, the problem is that θ_{t-0} for this surface can almost be neglected and the change in the surface coverage covers insignificant values. On the other hand, in the case of PS platinum the value $\Delta\theta$ is more than three-times larger than the reaction on pc platinum and also the value of I_{ss}. This means that the consumption of adsorbed species during the process on these surfaces is very important, however the value of $k_{\mathrm{ox},4}$ is lower (also three times lower) than on pc platinum, so a compensation effect is expected. Summing up, the product $\Delta\theta k_{\mathrm{ox},4}$ on both platinum surfaces is nearly the same and also the accumulation of adsorbed species on platinum/ruthenium and platinum/osmium, as it has been expected from the similar coverages obtained by each metal ad-atoms. To make further conclusions on the comparative value of θ a more advance model with a distinction between the initial methanol adsorbate and that of poisoning species is required.

Table 3
Values of $\Delta\theta k_{\mathrm{ox},4}$ (with $\Delta\theta \equiv \theta_{t=0} - \theta_{\mathrm{ss}}$), $\Delta\theta$ and I_{ss} (at 1800 s) from parameters of Tables 1 and 2 for chronoamperometric data at 0.70 V at platinum and metal modified surfaces; ruthenium, osmium, ruthenium:osmium and silver in 0.50 M methanol + 0.5 M sulphuric acid

	$\Delta\theta\, k_{\mathrm{ox},4}$ (s^{-1})	$\Delta\theta$	J_{ss} ($\mathrm{A\,cm}^{-2}$)
Pt	0.0173	1.58×10^{-8}	3.1×10^{-11}
Pt PS	0.0176	3.91×10^{-8}	7.0×10^{-11}
Pt Ru	0.0492	1.68×10^{-6}	3.0×10^{-21}
Pt Os	0.0099	3.82×10^{-9}	8.1×10^{-9}
Pt Ru Os	0.0061	6.50×10^{-6}	2.7×10^{-27}
Pt Ag	0.1200	1.28×10^{-3}	1.3×10^{-56}

6. Conclusions

(1) Chronoamperometric data were compared to envisage the catalytic effects of the different platinum surfaces towards methanol oxidation. The largest initial current density was observed for the cathodically treated surface; however, the asymptotic current showed a better response for platinum/osmium and ternary platinum/ruthenium/osmium.

(2) An initial current increase at 0.70 V was observed in the chronoamperometry for pc and cathodically treated platinum, because of the competitive initial carbon monoxide oxidation and methanol decomposition. However, platinum surfaces modified by a second metal spontaneously deposited always showed current transients with negative slopes, independent of the nature of the second metal. This suggests a possibility for minimising carbon monoxide formation.

(3) A theoretical analysis of the kinetic law for the proposed series mechanism of methanol electrocatalytic oxidation is presented here with an analytical solution of the differential equation solved using Ricatti's equation. The solution obeys a linear combination of exponentials (one of them related to carbon monoxide formation and the other to its oxidation). The fitting of the chronoamperometric data with the mathematical model, leads to an analysis of methanol decomposition and carbon monoxide oxidation.

(4) The time dependent expression of the surface coverage by methanol adsorbates is derived from the chronoamperometric data. The asymptotic value of the surface coverage, $\Delta\theta$, is inversely proportional to the electrochemical rate constant of the determining step. In the case of cathodically treated platinum, the value of $\Delta\theta$ is three-times larger than on pc platinum, indicating a large consumption of adsorbed species during the process. The values of $\Delta\theta$ on the metal modified platinum surfaces are lower except for platinum/silver where the methanol adsorption is strongly preferred.

(5) The value of the electrochemical rate-determining step was determined in all cases. The largest value was observed for platinum/ruthenium/osmium surface, i.e. $k_{ox,4} = 10^{-3}\ s^{-1}$, followed by platinum/ruthenium and platinum/osmium. The situation for platinum/silver is the worst with $k_{ox,4} = 5 \times 10^{-6}\ s^{-1}$. These results seem to be in contradiction with the large initial current obtained for cathodically treated and bare platinum. However, these surfaces are poisoned after long exposure times to methanol oxidation and the initial large currents get depressed.

Acknowledgements

The authors wish to thank S.M. and V. D. for the help with some measurements. PDT Project No. 16/02 has financially supported this work for the Energy Area at DINACYT (Uruguay). CFZ is a researcher at PEDECIBA-United Nations.

Appendix A. Ricatti's equation

The non-linear differential equation with quadratic terms

$$\frac{dy}{dx} = P(x) + Q(x)y + R(x)y^2 \tag{A1}$$

is called Ricatti's equation. If y_1 is a known particular solution of (A1), then the substitutions of

$$y = y_1 + u \quad \text{and} \quad \frac{dy}{dx} = \frac{dy_1}{dx} + \frac{du}{dx} \tag{A2}$$

in (A1) leads to the following differential equation for u:

$$\frac{du}{dx} - (Q + 2y_1R)u = Ru^2 \tag{A3}$$

Since (A3) is a Bernoulli equation with $n = 2$,

$$\frac{dy}{dx} + P(x)y = f(x)y^n, \tag{A4}$$

it in turn be reduced to the linear equation

$$\frac{dw}{dx} + (Q + 2y_1R)w = -R \tag{A5}$$

by the substitution $w \equiv u^{-1}$. The situation is that in many cases a solution of a Ricatti equation cannot be expressed in terms of elementary functions.

For example, if we have the following differential equation

$$\frac{dy}{dx} = 2 - 2xy + y^2 \tag{A6}$$

It can be easily verified that a particular solution of this equation is $y_1 = 2x$. From (A1) we make the identifications $P(x) = 2$, $Q(x) = -2x$, and $R(x) = 1$ and then solve the linear Eq. (6):

$$\frac{dw}{dx} + (-2x + 4x)w = -1 \quad \text{or} \quad \frac{dw}{dx} + 2xw = -1 \tag{A7}$$

The integrating factor for the last equation is e^{x^2}, so

$$\frac{d}{dx}(e^{x^2}w) = -e^{x^2} \tag{A8}$$

Now the integral

$$\int_{x_0}^{x} e^{t^2}\,dt \tag{A9}$$

cannot be expressed in terms of elementary functions. Thus, we write instead:

$$e^{x^2}w = -\int_{x_0}^{x} e^{t^2}\,dt + c \quad \text{or} \quad e^{x^2}\left(\frac{1}{u}\right) = -\int_{x_0}^{x} e^{t^2}\,dt + c \tag{A10}$$

so that

$$u = \frac{e^{x^2}}{c - \int_{x_0}^{x} e^{t^2}\,dt} \tag{A11}$$

A solution of the equation is then $y = 2x + u$.

Appendix B. The integration of the surface coverage by methanol adsorbates

The time dependence of the surface coverage by methanol adsorbates obeys:

$$\frac{d\theta}{dt} = \frac{N_A\sigma}{\Gamma_{sat}Fk_{ox,4}} \frac{C_1C_2(r_1 - r_2)^2 \exp((r_1 + r_2)t)}{(C_1\exp(r_1t) + C_2\exp(r_2t))^2} \tag{B1}$$

We can integrate it as follows:

$$\int_{\theta_i}^{\theta} d\theta = \frac{C_1C_2(r_1 - r_2)^2}{k_{ox,4}} \int_0^t \frac{\exp((r_1 + r_2)t)}{(C_1\exp(r_1t) + C_2\exp(r_2t))^2}\,dt \tag{B2}$$

or from

$$\int_{\theta_i}^{\theta} d\theta = -\frac{C_1C_2(r_1 - r_2)^2}{k_{ox,4}} \int_0^t \frac{\exp(r_1t)}{(C_2 + C_1\exp(r_1 - r_2)t)^2}\,dt \tag{B3}$$

By defining

$$\theta_o \equiv \frac{C_1C_2(r_1 - r_2)^2}{k_{ox,4}} \tag{B4}$$

$$\theta = \theta_i - \theta_o \int_0^t \frac{\exp(r_1 - r_2)t}{(C_1 + C_2\exp(r_1 - r_2)t)^2}\,dt \tag{B5}$$

We can use the Substitution Theorem for integration. If $t = g(x)$ is a derivable function and has an inverse function $x = a(t)$, and if $f(g(x))g'(x)$ has a primitive function, it is possible to say that the primitive of f(t) will be $\int f(t)dt = \int f(g(x))g'(x)dx$.

In our case, we have:

$$f(t) \equiv \frac{\exp(r_1 - r_2)t}{(C_1 + C_2\exp(r_1 - r_2)t)^2} \tag{B6}$$

If $t = g(x) \equiv 1/(r_1 - r_2)\ln x$ then: $x = \exp(r_1 - r_2)t$ and $g'(x) \equiv 1/(r_1 - r_2)x$. By substituting the new variables in the

primitive of $f(t)$

$$\int f(t)\mathrm{d}t = \frac{1}{(r_1 - r_2)} \int \frac{1}{(C_1 + C_2 x)^2}\mathrm{d}x \tag{B7}$$

Therefore, we can integrate now as:

$$\frac{1}{(r_1 - r_2)} \int \frac{1}{(C_1 + C_2 x)^2}\mathrm{d}x = \frac{1}{C_2(r_1 - r_2)} \left[\frac{-1}{(C_1 + C_2 x)}\right]_{x1}^{x2} \tag{B8}$$

since the integration limits are $x_1 = \exp(r_1 - r_2)t_1 = 1$ (t_1 is the zero initial time) and $x_2 = \exp(r_1 - r_2)t_2$

$$\int f(t)\mathrm{d}t = \frac{1}{C_2(r_1 - r_2)} \times \left[\frac{1}{(C_1 + C_2)} - \frac{1}{(C_1 + C_2 \exp(r_1 - r_2)t)}\right] \tag{B9}$$

We can obtain now the surface coverage by the final substitution:

$$\theta = \theta_i - \frac{C_1(r_1 - r_2)}{k_{\mathrm{ox},4}} \times \left[\frac{1}{(C_1 + C_2)} - \frac{1}{(C_1 + C_2 \exp(r_1 - r_2)t)}\right] \tag{B10}$$

References

[1] E. Entchev, J. Power Sources 118 (2003) 212.
[2] P. Kruger, Int. J. Hydrogen Energy 26 (2001) 1137.
[3] R.A. Lemons, J. Power Sources 29 (1990) 251.
[4] L. Carrette, K.A. Friedrich, U. Stimming, Fuel Cells 1 (2001) 5.
[5] V.S. Bagotzki, Y.B. Vassilev, Electrochim. Acta 12 (1967) 1323.
[6] R. Indara, K. Shimazu, H. Kita, J. Electroanal. Chem. 277 (1990) 315.
[7] H.A. Gasteiger, N. Markovic, P.N. Ross, E.J. Cairns, J. Phys. Chem. 97 (1993) 46.
[8] H. Massong, H. Wang, G. Samjeskė, H. Baltruschat, Electrochim. Acta 46 (2000) 701.
[9] M. Watanabe, S. Motoo, J. Electroanal. Chem. 60 (1975) 275.
[10] S. Mukerjee, S.J. Lee, E.A. Ticianelli, J. McBreen, B.N. Grgur, N.M. Markovic, P.N. Ross, J.R. Giallombardo, E.S. de Castro, Electrochem. Solid State Lett. 2 (1999) 12.
[11] B. Hammer, J.K. Nørskov, Adv. Catal. 45 (2000) 71.
[12] K. Franaszczuk, E. Herrero, P. Zelenay, A. Wieckoswski, J. Wang, R.I. Masel, J. Phys. Chem. 96 (1992) 8509.
[13] E. Herrero, K. Franaszczuk, A. Wieckoswski, J. Phys. Chem. 98 (1994) 5074.
[14] G. Stab, P. Urban, US Patent 6 (2001) 258, 239.
[15] S.H. Bonilla, C.F. Zinola, J. Rodríguez, V. Díaz, M. Ohanian, S. Martínez, B. Gianetti, J. Colloid Interface Sci. 288 (2005) 377.
[16] P. Waszczuk, G.-Q. Lu, A. Wieckoswski, C. Lu, C. Rice, R.I. Masel, Electrochim. Acta 47 (2002) 3637.
[17] Y. Ishikawa, M. Liao, C.R. Cabrera, Surf. Sci. 463 (2000) 66.
[18] Z.D. Wei, S.H. Chan, J. Electroanal. Chem. 569 (2004) 23.
[19] A.J. Dickinson, L.P.L. Carrette, J.A. Collins, K.A. Friedrich, U. Stimming, Electrochim. Acta 47 (2002) 3733.
[20] S. Wasmus, A. Kuver, J. Electroanal. Chem. 461 (1999) 14.
[21] H. Hoster, T. Iwasita, H. Baumgartner, W. Vielstich, Phys. Chem. Chem. Phys. 3 (2001) 337.
[22] C. Bock, B. MacDougall, Y. LePage, J. Electrochem. Soc. 151 (2004) A1269.
[23] J.W. Long, R.M. Stroud, K.E. Swider-Lyons, D.R. Rolison, J. Phys. Chem. B 104 (2000) 9772.
[24] H.N. Dinh, X. Ren, F.H. Garzon, P. Zelenay, S. Gottesfeld, J. Electroanal. Chem. 491 (2000) 222.
[25] H. Kim, I.R. deMoraes, G. Tremiliosi, R. Haasch, A. Wieckowski, Surf. Sci. 474 (2001) L203.
[26] C. Bock, B. MacDougall, J. Electrochem. Soc. 150 (2003) 377.
[27] S. Sriramulu, T.D. Jarvi, E.M. Stuve, J. Electroanal. Chem. 467 (1999) 132.
[28] T.D. Jarvi, S. Sriramulu, E.M. Stuve, J. Phys. Chem. B 101 (1997) 3649.
[29] T.D. Jarvi, S. Sriramulu, E.M. Stuve, Colloids Surf. A 134 (1998) 145.
[30] X.H. Xia, T. Iwasita, F. Ge, W. Vielstich, Electrochim. Acta 41 (1996) 711.
[31] S. Sriramulu, T.D. Jarvi, E.M. Stuve, Electrochim. Acta 44 (1998) 1127.
[32] L.D. Burke, L.M. Hurley, Electrochim. Acta 44 (1999) 3451.
[33] V. Díaz, M. Ohanian, B. Gualtieri, C.F. Zinola, in revision.
[34] M. Janssen, J. Moolhuysen, Electrochim. Acta 21 (1976) 861.
[35] E. Spinacé, A. Neto, M. Linardi, J. Power Sources 129 (2004) 121.
[36] A. Crown, C. Johnston, A. Wieckowski, Surf. Sci. 506 (2002) L268.
[37] S. Strbac, C. Johnston, G. Lu, A. Crown, A. Wieckowski, Surf. Sci. 573 (2004) 80.
[38] V. Colle, M. Giz, G. Tremiliosi Filhio, J. Braz. Chem. Soc. 14 (2003) 601.
[39] P.A. Thiel, T.E. Madey, Surf. Sci. Rep. 7 (1987) 211.
[40] N.M. Marković, P.N. Ross Jr., Surf. Sci. Rep. 45 (2002) 117.
[41] J.W. Ndieyira, A.R. Ramadan, T. Rayment, J. Electroanal. Chem. 503 (2001) 28.
[42] D. Oyamatsu, H. Kanemoto, S. Kuwabata, H. Yoneyama, J. Electroanal. Chem. 497 (2001) 97.
[43] M.C. Santos, L.H. Mascaro, S.A.S. Machado, Electrochim. Acta 43 (1998) 2263.
[44] D.M. Kolb, Surf. Sci. 500 (2002) 722.
[45] M.E. Martins, R.C. Salvarezza, A.J. Arvia, Electrochim. Acta 41 (1996) 2441.
[46] J.C. Davies, B.E. Hayden, D.J. Pegg, M.E. Rendall, Surf. Sci. 496 (2002) 110.
[47] P. Waszczuck, J. Solla-Guillon, H.S. Kim, Y.Y. Tong, V. Montiel, A. Aldaz, A. Wieckowski, J. Catal. 203 (2001) 1.
[48] T. Iwasita, H. Hoster, A. John-Anacker, W.F. Lin, W. Vielstich, Langmuir 16 (2000) 522.
[49] P. Waszczuck, T.M. Barnard, C. Rice, R.I. Masel, A. Wieckowski, Electrochem. Commun. 4 (2002) 599.
[50] A. Crown, I. de Moraes, A. Wieckowski, J. Electroanal. Chem. 500 (2001) 333.
[51] A. Crown, A. Wieckowski, Phys. Chem. Chem. Phys. 3 (2001) 3290.
[52] A. Hamnett, B.J. Kennedy, F.E. Wagner, J. Catal. 124 (1990) 30.
[53] R. Liu, H. Iddir, Q. Fan, G. Hou, A. Bo, K.L. Ley, E.S. Smotkin, Y.E. Sung, H. Kim, S. Thomas, A. Wieckowski, J. Phys. Chem. B 104 (2000) 3518.
[54] V. Diaz, M. Ohanian, B. Gualtieri, C.F. Zinola, J. Colloid Interface Sci., in revision.
[55] R. Parsons, T. VanderNoot, J. Electroanal. Chem. 257 (1988) 9.
[56] E. Herrero, W. Chrzanowski, A. Wieckoswski, J. Phys. Chem. 99 (1995) 10423.
[57] G.Q. Lu, W. Chrzanowski, A. Wieckowski, J. Phys. Chem. B 104 (2000) 5566.
[58] W. Vielstich, X.H. Xia, J. Phys. Chem. 99 (1995) 10421.
[59] H. Wang, T. Lőffler, H. Baltruschat, J. Appl. Electrochem. 31 (2001) 759.
[60] T.H.M. Housmans, M.T.M. Koper, J. Phys. Chem. B 107 (2003) 8557.
[61] W. Reid, Ricatti differential equations, in: Mathematics in Science and Engineering, 86, Academic, New York, 1972.

Glossary

c: the surface concentration in (mol cm^{-2})
F: the Faraday's constant (C mol^{-1})
j(t): the time dependent current density (A cm^{-2})
K, L and M: parametric terms of the Ricatti equation (cm^2 mol^{-1} s^{-1}) with $K \equiv F/\sigma[(4-x)k_{\mathrm{red},2}(\mathrm{H}^+)^{4-x} - (4-x)k_{\mathrm{ox},2} + xk_{\mathrm{red},1}(\mathrm{H}^+)^x - k_{\mathrm{red},3}(\mathrm{H}^+)]$, $L \equiv Fk_{\mathrm{ox},4}/\sigma$, $M \equiv F/\sigma[k_{\mathrm{ox},3} - (4-x)k_{\mathrm{ox},1}(\mathrm{CH_3OH})]$

$k_{ox,i}$ *and* $k_{red,i}$: the electrochemical rate constants for each oxidation and reduction pathways (s^{-1})
n: the number of electrons
N_A: the Avogadro's number (molecules mol^{-1})
p_i: the reaction order for bulk and surface concentrations of reactants
t_{ss}: the steady state time at which the variation of the current density is zero
$\vec{v}$: the electrochemical rate of reaction (mol cm^{-2} s^{-1})
σ: the maximum surface charge density in (C cm^{-2})
θ: surface coverage by adsorbed intermediates in methanol oxidation
θ_i: the initial surface coverage by methanol adsorbates ($t \to 0$)
θ_{ss}: the value of surface coverage at steady state ($t \to \infty$)
$\Delta\theta$: the integral change in the surface coverage equal to $\theta_{ss} - \theta_{t-0}$
Δ: the pre-exponential factor of the current density defined as $\Delta \equiv \sigma C_1 C_2 (r_1 - r_2)^2 / k_{ox,4}$, C_1 and C_2 (dimensionless) being the pre-exponential factors of the linear combination in the solution of Ricatti expression, and r_1 and r_2 (s^{-1}) the exponential terms in the same solution
Γ *and* Γ_{sat}: the surface excess at any time and at under saturation conditions in (molecules cm^{-2}) with $\Gamma_{sat} = N_A \sigma / F$